This article was downloaded by: [Tomsk State University of Control Systems and Radio]
On: 18 February 2013, At: 14:17
Publisher: Taylor & Francis
Informa Ltd Registered in England and Wales Registered Number: 1072954 Registered office: Mortimer House, 37-41 Mortimer Street, London W1T 3JH, UK

Molecular Crystals and Liquid Crystals Science and Technology. Section A. Molecular Crystals and Liquid Crystals
Publication details, including instructions for authors and subscription information:
http://www.tandfonline.com/loi/gmcl19

A New Measurement of Second-Harmonic Generation Efficiency

Masashi Kiguchi [a], Midori Kato [a], Nami Kumegawa [a] & Yoshio Taniguchi [a]
[a] Advanced Research Laboratory, Hitachi Ltd., Hatoyama, Saitama, 350-03, Japan
Version of record first published: 24 Sep 2006.

To cite this article: Masashi Kiguchi , Midori Kato , Nami Kumegawa & Yoshio Taniguchi (1993): A New Measurement of Second-Harmonic Generation Efficiency, Molecular Crystals and Liquid Crystals Science and Technology. Section A. Molecular Crystals and Liquid Crystals, 227:1, 133-142

To link to this article: http://dx.doi.org/10.1080/10587259308030966

PLEASE SCROLL DOWN FOR ARTICLE

Full terms and conditions of use: http://www.tandfonline.com/page/terms-and-conditions

This article may be used for research, teaching, and private study purposes. Any substantial or systematic reproduction, redistribution, reselling, loan, sub-licensing, systematic supply, or distribution in any form to anyone is expressly forbidden.

The publisher does not give any warranty express or implied or make any representation that the contents will be complete or accurate or up to date. The accuracy of any instructions, formulae, and drug doses should be independently verified with primary sources. The publisher shall not be liable for any loss, actions, claims, proceedings, demand, or costs or damages whatsoever or howsoever caused arising directly or indirectly in connection with or arising out of the use of this material.

Mol. Cryst. Liq. Cryst. 1993, Vol. 227, pp. 133–142
Reprints available directly from the publisher
Photocopying permitted by license only
© 1993 Gordon and Breach Science Publishers S.A.
Printed in the United States of America

Downloaded by [Tomsk State University of Control Systems and Radio] at 14:17 18 February 2013

A NEW MEASUREMENT OF SECOND-HARMONIC GENERATION EFFICIENCY

MASASHI KIGUCHI, MIDORI KATO, NAMI KUMEGAWA,
and YOSHIO TANIGUCHI
Advanced Research Laboratory, Hitachi Ltd., Hatoyama, Saitama 350-03, Japan

Abstract A new method of measuring second-harmonic generation efficiency using powder crystals is demonstrated. The second-harmonic wave generated with the evanescent wave (SHEW) is phase-matched for every material. The efficiency of the second-harmonic generation can be estimated from the SHEW power, regardless of the phase-matchability of the material in a bulk crystal, even when powder crystals are used as the sample.

INTRODUCTION

Second-harmonic generation (SHG) has been used to extend the wavelength of lasers. With the development of diode lasers, SHG is expected to lead to a compact visible light source that will be used in optical memories and optical experiments. Organic materials with conjugated π-electron donors and acceptors are expected as the SHG materials because of their large nonlinearity and their variety of synthesis. A number of organic nonlinear optical materials have been synthesized and surveyed. The powder measurement[1] is a well-known method for evaluating these new materials. The second-harmonic output from powder crystals irradiated by a laser is observed in this measurement. Because the powder measurement is simple and has the great advantage of not requiring large crystals, it is often used to estimate the nonlinear optical constants of a crystal. The second-harmonic intensity measured by the powder method depends on the particle size and the phase-matching condition of the powder crystals. The second-harmonic output must be measured as a function of the ratio of the particle size to the coherence length. However, it is frequently difficult to make particles as small as the coherence length. When the average particle size of the powder is much larger than the coherence length, the nonlinear optical constant of the non-phase-matchable material is estimated smaller than the true value. In practice, such non-phase-matchable materials can actually be used in the waveguide structure[2], so many promising materials may have been previously overlooked in the surveys.

We have proposed a new method of evaluating SHG materials using powder crys-

tals. The second-harmonic wave generated with the evanescent wave (SHEW) is observed in total reflection, which is automatically phase-matched. The SHEW intensity is simply proportional to the figure of merit which shows the SHG efficiency, whether the material is phase-matchable or not. This method gives more accurate results than the conventional powder method. This article presents a more complete theoretical treatment than our previous letter[3], and the measurement data is refined. Hereafter we call this measurement the SHEW method.

THEORY

Most nonlinear optical effects have complexity related to the phase-matching conditions, because the velocity of the generated light is different from that of the nonlinear polarization due to the dispersion of the refractive indices. The second-harmonic intensity measured by the powder method also depends on the phase-matching conditions. It depends on the phase-matchability and the ratio of the average particle size to the average coherence length ℓ_c, defined by

$$\ell_c = \pi c / \omega \left(n^{2\omega} - n^{\omega} \right). \tag{1}$$

Therefore, it is not simply proportional to the figure of merit M_{ij}, defined by

$$M_{ij} = \frac{d_{ij}^2}{n^{2\omega} \left(n^{\omega} \right)^2}. \tag{2}$$

Here, d_{ij} is the ij th element of the second-order nonlinear coefficient tensor and n is the refractive index of the material. This is one of the main reasons why the powder method gives poor results. If the phase-matching condition is always satisfied with any sample by the measurement, the results will be more accurate. This occurs with total reflection.

We consider the boundary between a linear medium with an incident wave and a nonlinear medium (Figure 1). When the fundamental wave is totally reflected, the evanescent wave, whose frequency is ω, propagates along the boundary, and decreases exponentially away from the boundary. The phase velocity of the evanescent wave is given by

$$v_e = \omega / \left(n_p^{\omega} k_0 \sin \theta_{in} \right), \tag{3}$$

where θ_{in} is the incidence angle of the fundamental wave, n_p^{ω} is the refractive index of the

Downloaded by [Tomsk State University of Control Systems and Radio] at 14:17 18 February 2013

linear medium at frequency ω, and k_0 is the wave number of the fundamental wave[4]. The nonlinear polarization, whose frequency is 2ω, also propagates along the boundary at the same velocity, and its amplitude decreases exponentially away from the boundary. The second-harmonic wave radiates into the linear medium. Every phase of the second-harmonic wave is matched when the following condition is satisfied.

$$v_e \sin\theta_m = v_{SH} = 2\omega/\left(2k_0 n_p^{2\omega}\right). \tag{4}$$

Equations (3) and (4) reduce to

$$n_p^{\omega} \sin\theta_{in} = n_p^{2\omega} \sin\theta_m. \tag{5}$$

Here, $n_p^{2\omega}$ is the refractive index of the linear medium at frequency 2ω. Because Eq. (5) has no parameter related to the nonlinear material, the second-harmonic wave is always phase-matched with any sample and radiates towards θ_m, which depends on the incidence angle and the refractive indices of the linear medium. Therefore, when a sample is placed in contact with a prism that has a high refractive index, we can get the figure of merit of the sample by observing the second-harmonic intensity, whether or not the sample is phase-matchable in a bulk crystal. In order to simplify the treatment, the birefringence of the prism and the sample are not considered here. It will be shown later that this approximation gives reasonable results. The SHEW method has the advantage that it is not necessary to change the set-up according to the sample, because θ_m is independent of the sample.

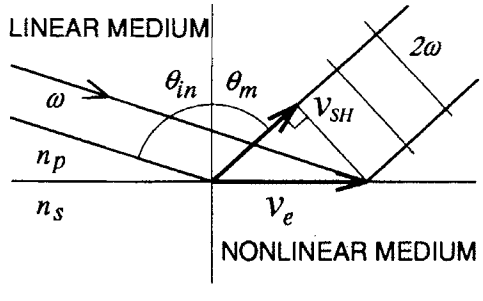

FIGURE 1 Phase-matching of the second-harmonic wave with the evanescent wave.

Downloaded by [Tomsk State University of Control Systems and Radio] at 14:17 18 February 2013

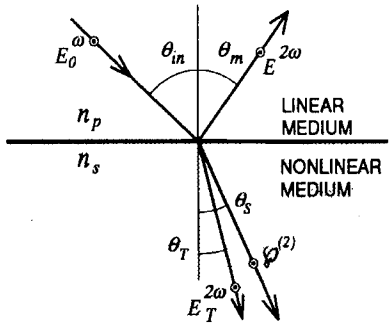

FIGURE 2 Schematic diagram describing the second-harmonic generation with a semi-infinite nonlinear medium with a boundary surface.

The second-harmonic power obtained by this measurement was described approximately in our previous paper[3]. Our model was an adequate approximation when the dispersion of the refractive index of the sample was negligible and the range of θ_{in} was small. Here, we give a more accurate treatment. The general treatment of the light waves at the boundary of a nonlinear medium was described by Bloembergen *et al.*[5] Their results can be applied to our problem. We now consider the fundamental wave with s-polarization and the second-harmonic output with s-polarization (Figure 2). The continuity conditions of the electric field E and the magnetic field H at the boundary are written as

$$E^{2\omega} = E_T^{2\omega} + 4\pi\wp^{(2)} \Big/ \left[\left(n_s^{\omega}\right)^2 - \left(n_s^{2\omega}\right)^2 \right], \tag{6}$$

$$\begin{aligned} H^{2\omega} &= -n_p^{2\omega} E^{2\omega} \cos\theta_m \\ &= n_s^{2\omega} E_T^{2\omega} \cos\theta_T + 4\pi n_s^{\omega} \wp^{(2)} \cos\theta_S \Big/ \left[\left(n_s^{\omega}\right)^2 - \left(n_s^{2\omega}\right)^2 \right], \end{aligned} \tag{7}$$

where $E_T^{2\omega}$ is the electric field amplitude of the transmitted harmonic wave propagating in the direction defined by angle θ_T, which is obtained by Snell's law, and $\wp^{(2)}$is the second-order nonlinear polarization propagating in the direction defined by angle θ_S. Equations (6) and (7) reduce to

$$E^{2\omega} = -\frac{4\pi\wp^{(2)}}{\left(n_s^{2\omega}\cos\theta_T + n_s^{\omega}\cos\theta_S\right)\left(n_s^{2\omega}\cos\theta_T + n_p^{2\omega}\cos\theta_m\right)}. \tag{8}$$

Downloaded by [Tomsk State University of Control Systems and Radio] at 14:17 18 February 2013

Downloaded by [Tomsk State University of Control Systems and Radio] at 14:17 18 February 2013

We have two critical angles, θ_c and θ_{c2}, defined as

$$\sin\theta_c = \frac{n_s^{\omega}}{n_p^{\omega}}, \tag{9}$$

$$\sin\theta_{c2} = \frac{n_s^{2\omega}}{n_p^{\omega}}. \tag{10}$$

The fundamental wave is totally reflected, and the transmitted second-harmonic wave propagates in the nonlinear medium, when $\theta_c < \theta_{in} < \theta_{c2}$. In this case, $\cos\theta_S$ is purely imaginary. This means that nonlinear polarization is induced by the evanescent wave. When $\theta_{c2} < \theta_{in}$, $\cos\theta_T$ is purely imaginary, i.e., the transmitted second-harmonic wave cannot propagate in the nonlinear medium. The nonlinear polarization $\wp^{(2)}$ induced by the evanescent wave is written as

$$\wp^{(2)} = d : E_{ev}E_{ev},$$

$$\begin{aligned} E_{ev} &= \frac{2E_0^{\omega} n_p^{\omega}\cos\theta_{in}}{n_p^{\omega}\cos\theta_{in} + n_s^{\omega}\cos\theta_S} \\ &= \frac{2E_0^{\omega}\cos\theta_{in}}{\cos\theta_{in} + i\sqrt{\sin^2\theta_{in} - \left(n_s^{\omega}/n_p^{\omega}\right)^2}}. \end{aligned} \tag{11}$$

The SHEW power is given by

$$P_{SHEW} = \frac{cn_p^{2\omega}}{8\pi}\frac{\cos\theta_m}{\cos\theta_{in}}A \times \left| \frac{4\pi\wp^{(2)}}{\left(n_s^{2\omega}\cos\theta_T + i\sqrt{\left(n_p^{\omega}\right)^2\sin^2\theta_{in} - \left(n_s^{\omega}\right)^2}\right)\left(n_s^{2\omega}\cos\theta_T + n_p^{2\omega}\cos\theta_m\right)} \right|^2 \tag{12}$$

where A is the incident beam cross section. This is proportional to d^2 and has no term related to the phase-matching. The measurement of the SHEW power from the sample relative to that from the reference sample gives the relative value of the figure of merit without the complexity of phase-mismatching. The scattering of the second-harmonic wave from bulk crystals can be reduced when $\theta_{c2} < \theta_{in}$.

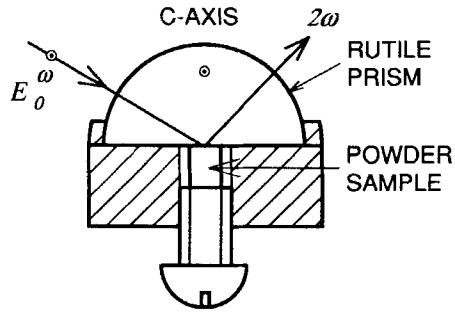

FIGURE 3 Schematic layout of the prism and the powder sample. Powder crystals are pushed into contact with the rutile prism by the screw. Polarization of the incident wave is parallel to the c-axis of the rutile crystal.

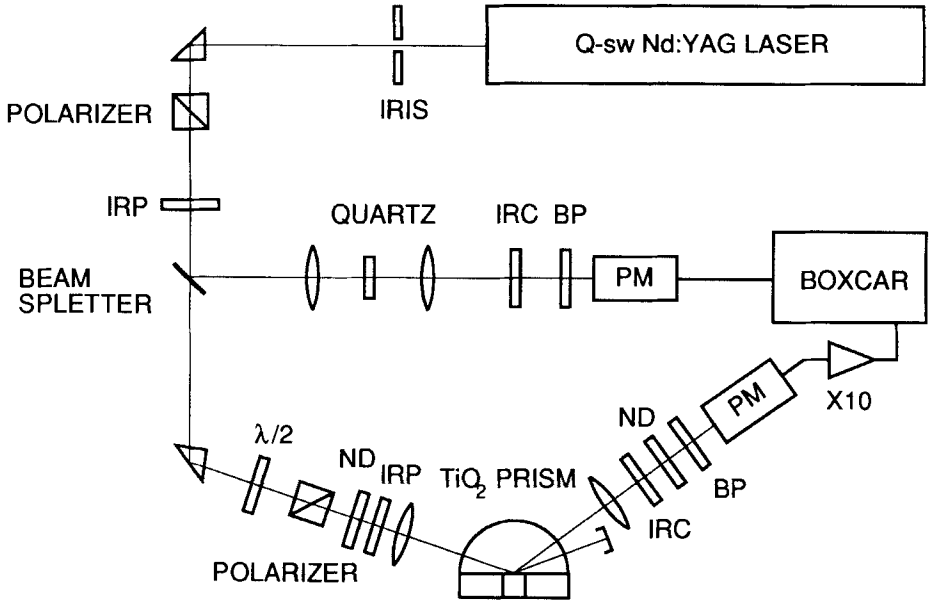

FIGURE 4 Experimental arrangement of the SHEW method. IRP, IRC, ND, and BP represent Infrared (IR) pass, IR cut, Neutral density, and Band pass filters, respectively.

Downloaded by [Tomsk State University of Control Systems and Radio] at 14:17 18 February 2013

Downloaded by [Tomsk State University of Control Systems and Radio] at 14:17 18 February 2013

EXPERIMENTS AND RESULTS

The schematic layout of the prism and sample is shown in Figure 3. The prism has a hemicylindrical shape in order to avoid any change in incidence angle with refraction. Powder crystals are pushed into contact with the prism by the screw. Since the prism is made of rutile (TiO_2) crystal, which has large refractive indices[6], n_p^{ω}=2.74 and $n_p^{2\omega}$=2.98, the total reflective condition is satisfied for almost any sample. The polarization of the fundamental wave is parallel to the c-axis of the rutile crystal so that it dose not change due to birefringence.

The experimental arrangement for the SHEW method is shown in Figure 4. A Q-switched Nd:YAG laser was driven at 30 Hz, producing optical pulses with a wavelength of 1.06 μm. The fundamental beam was split into two beams by a beamsplitter. One passed through a quartz crystal to provide a reference second-harmonic power for the calibration of the fundamental beam power. The other was attenuated by filters and guided into the prism. The beam was focused on the front of the prism to be collimated in the prism. The prism could be rotated using a stepping-motor-driven stage to scan the incidence angle. The second-harmonic output was collimated and detected by a photo-multiplier after the scattered fundamental wave was removed by short-wavelength-passing filters and a band pass filter. Neutral density filters were used to control the signal intensity in the dynamics range of the system. These components were arranged on another stepping-motor-driven rotational stage to adjust the observation angle. The signal from the photomultiplier was amplified by ten times with a preamplifier and averaged with a boxcar averager. The two stepping motors and the boxcar averager were controlled with a computer (HP 360).

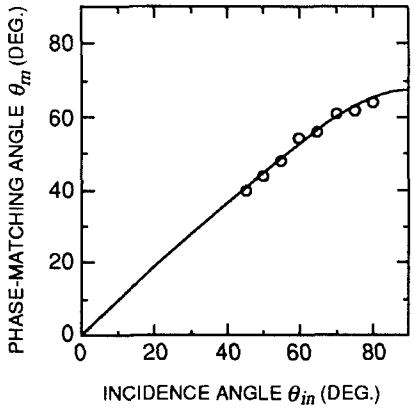

FIGURE 5 Phase-matching angle of the SHEW as a function of the incidence angle of the fundamental wave. Sample is the MNA powder.

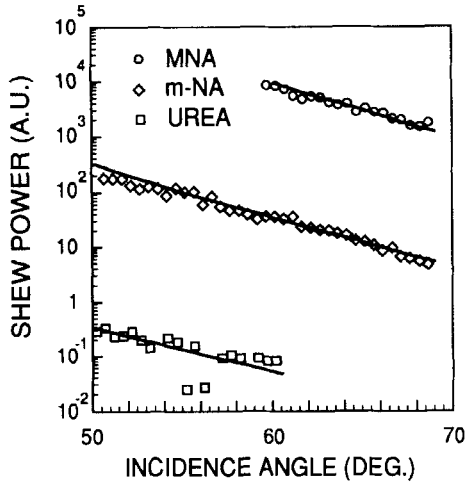

FIGURE 6 SHEW power from the powder samples at the various incidence angles. The curves are fit by the least squares method.

To confirm Eq. (5), the angles that gave strong second-harmonic output were measured at various incidence angles (Figure 5). For this measurement, the slit was arranged on the front of the lens in the output direction. The accuracy of the observation angle was estimated to be 0.5 degrees. As the signal had a broad peak, the peak angles were plotted. The circles represent the experimental results and the solid curve represents the phase-matching angles calculated by Eq. (5). Here powder crystals of 2-methyl-4-nitroaniline (MNA) were used as a sample. The observed values agreed well with the calculated ones.

The SHEW powers were measured for MNA, meta-nitroaniline (m-NA), and urea powder crystals as a function of the incidence angle. The results are shown in Figure 6. The curves were calculated by Eq. (12) and fit with the experimental data by the least squares method. The SHEW has also p-polarization, because d is a tensor and the crystals are randomly oriented. Although only s-wave was considered in Eq. (12), adequate fitting was possible with the effective refractive indices. The effective d or the effective figure of merit can be obtained as one of the fitting parameters. The particle sizes of the sample were not standardized. They ranged from 10 to 100 μm. The signal intensity did not depend on the particle size. Conventional powder measurement was also done for comparison using the same samples.

DISCUSSION

The figures of merit for these materials were precisely measured using single crystals by

Downloaded by [Tomsk State University of Control Systems and Radio] at 14:17 18 February 2013

the Maker fringe measurement, etc. The figures of merit for powders and single crystals are compared in Figure 7. The horizontal axis shows the value of the largest element of the figure of merit measured using a single crystal for each material in the references[7-9]. The vertical axis shows the figure of merit measured using powder crystals. Here, the results of the conventional powder method are calculated on the assumption that the signal intensity is simply proportional to the figure of merit. As each value is normalized to that of urea, both values are expected to be equal, i.e., the results will be plotted on a straight line. The results of the SHEW method represented by circles are closer to the line than the results of the conventional powder method represented by crosses. The powder method is therefore less reliable than the SHEW method. The phase-matchability of the materials gives inadequate results using the conventional powder method, because the phase-matchable elements of the figure are dominant. On the other hand, the large elements dominate the result by the SHEW method. Observing the reflected nonlinear wave can always avoid this complexity. The scattering of the second-harmonic wave from bulk crystals, whose intensity is dependent on the phase-matchability, can be suppressed, however, by using total reflection. Thus using total reflection plays an important role in getting reasonable results.

The obtained figures of merit are effective values, because the orientations of the

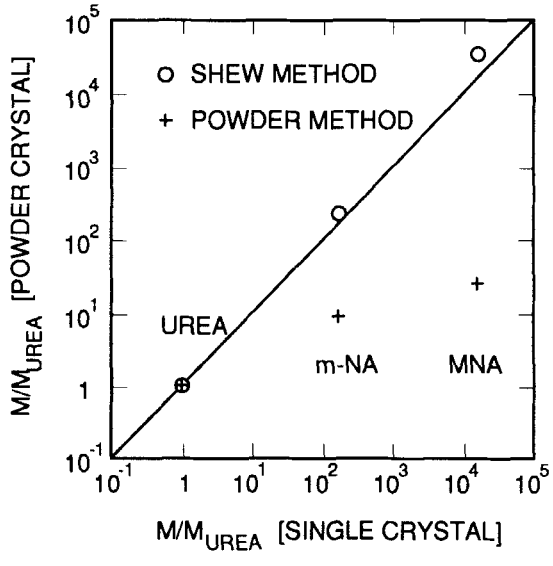

FIGURE 7 Comparison of the relative figures of merit by various measurements. The values by the SHEW method are closer to the values measured using single crystals than the values by the powder method.

Downloaded by [Tomsk State University of Control Systems and Radio] at 14:17 18 February 2013

powder crystals were not controlled. In principal, they are different from the value of the largest element of the figure of merit tensor. The signal intensity will depend on the packing densities of the samples. Moreover, The scattering of the fundamental wave at the interface will lead to errors in the results because of the use of powder samples. Although the SHEW method has some problems, as mentioned above, it gives surprisingly good results. The scattering and variation in the packing densities can be suppressed by controlling the contact pressure between the prism and the powders. Additional experiments are in progress to determine the best measurement conditions and these will be reported with the applications to other samples.

CONCLUSIONS

We have demonstrated a new method of evaluating SHG materials using powder crystals. The second-harmonic wave generated with the evanescent wave is always phase-matched. The SHEW power is proportional to the figure of merit of the material, whether the material is phase-matchable or not. The SHEW method gave better results than the conventional powder method for some popular SHG materials.

With the recent success in using laser diodes made from II-VI semiconductors to produce blue-green light[10] and its rapid development, the study of SHG materials needs to be accelerated. The SHEW method will be a powerful tool for developing new materials, and systematic experiments will provide guidelines for this development. This method can be used for materials that are difficult to grow as large crystals. If promising materials are discovered, it will stimulate the study of crystal growth and the development of new devices.

REFERENCES

1. S. K. Kurtz and T. T. Perry, J. Appl. Phys., 39, 3798 (1968).
2. J. D. Bierlein, D.B. Laubacher, J. B. Brown, and C. J. van der Poel, Appl. Phys. Lett., 56, 1725 (1990).
3. M. Kiguchi, M. Kato, M. Okunaka, and Y. Taniguchi, Appl. Phys. Lett., 60, 1935 (1992).
4. M. Born and E. Wolf, Principles of Optics (Pergamon, Oxford, 1975), pp. 47.
5. N. Bloembergen and P. S. Pershan, Phys. Rev., 128, 606 (1962).
6. J. R. DeVore, J. Opt. Soc. Am., 41, 418 (1951).
7. B. F. Levine, C. G. Bethea, C. D. Thurmond, R. T. Lynch, and J. L. Bernstein, J. Appl. Phys., 50, 2523 (1979).
8. A. Carenco, J. Jerphagnon, and A. Perigaud, J. Chem. Phys., 66, 3806 (1977).
9. J.-M. Halbout, S. Blit, W. Donaldson, and C. L. Tang, IEEE J. Quantum Electron., QE-15, 1176 (1979).
10. M. A. Haase, J. Qiu, J. M. DePuydt, and H. Cheng, Appl. Phys. Lett., 59, 1272 (1991).

Downloaded by [Tomsk State University of Control Systems and Radio] at 14:17 18 February 2013